nature chemical biology

SUPPLEMENTARY INFORMATION
https://doi.org/10.1038/s41589-018-0200-7

In the format provided by the authors and unedited.

Discovery of a ZIP7 inhibitor from a Notch pathway screen

Erin Nolin[1,5], Sara Gans[1,5], Luis Llamas[1], Somnath Bandyopadhyay[1], Scott M. Brittain[1], Paula Bernasconi-Elias[1], Kyle P. Carter[2], Joseph J. Loureiro[1], Jason R. Thomas[1], Markus Schirle[1], Yi Yang[1], Ning Guo[1], Guglielmo Roma[3], Sven Schuierer[3], Martin Beibel[3], Alicia Lindeman[1], Frederic Sigoillot[1], Amy Chen[1], Kevin X. Xie[1], Samuel Ho[1], John Reece-Hoyes[1], Wilhelm A. Weihofen[1], Kayla Tyskiewicz[1], Dominic Hoepfner[3], Richard I. McDonald[1], Nicolette Guthrie[1], Abhishek Dogra[1], Haibing Guo[4], Jian Shao[1], Jian Ding[1], Stephen M. Canham[1], Geoff Boynton[1], Elizabeth L. George[1], Zhao B. Kang[1], Christophe Antczak[1], Jeffery A. Porter[1], Owen Wallace[1], John A. Tallarico[1], Amy E. Palmer[2], Jeremy L. Jenkins[1], Rishi K. Jain[1], Simon M. Bushell[1,6*] and Christy J. Fryer[1,6*]

[1]Novartis Institutes for Biomedical Research, Cambridge, MA, USA. [2]Department of Chemistry and Biochemistry and BioFrontiers Institute, University of Colorado, Boulder, CO, USA. [3]Novartis Institutes for Biomedical Research, Basel, Switzerland. [4]Novartis Institutes for Biomedical Research, Shanghai, China. [5]These authors contributed equally: Erin Nolin, Sara Gans. [6]These authors jointly supervised this work: Simon M. Bushell, Christy J. Fryer.
*e-mail: simon.bushell@novartis.com; christy.fryer@novartis.com

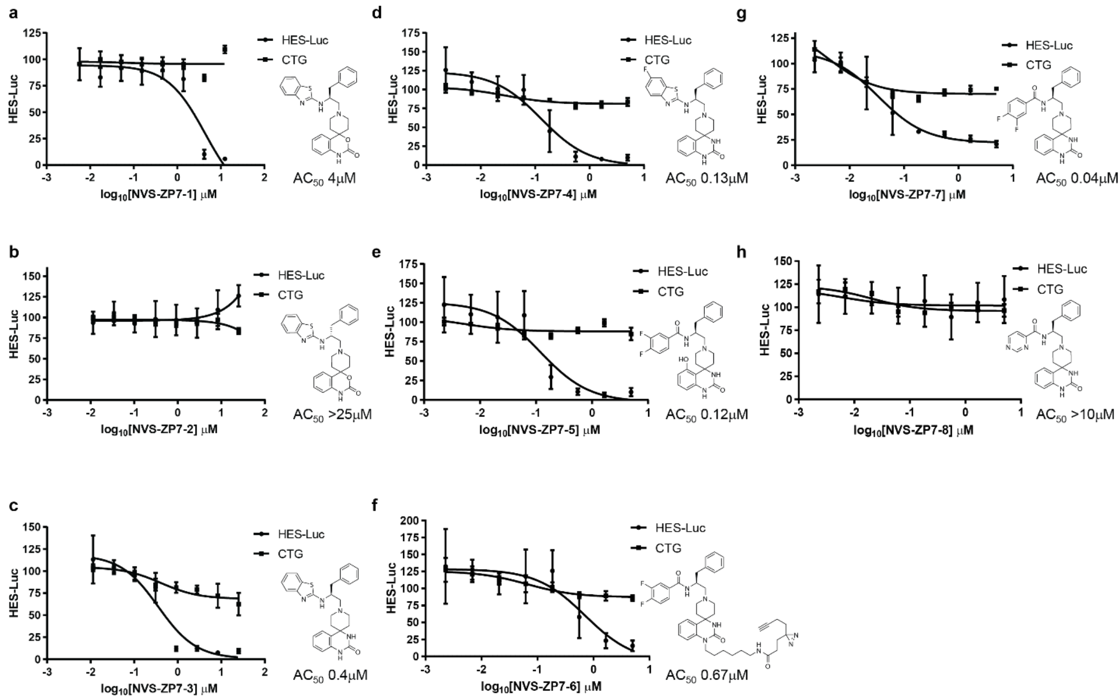

Supplementary Figure 1. Structure of NVS-ZP7 compounds and activity in Notch signaling HES-Luc reporter gene assay as well as the CTG counter screen. (a) Dose response of NVS-ZP7-1 in HES-Luc and CTG assays and compound structure. Error bars are standard deviation of the mean from 6 technical replicates. Each experiment was performed two independent times (b) Data for NVS-ZP7-2 (c) Data for NVS-ZP7-3 (d) Data for NVS-ZP7-4 (e) Data for NVS-ZP7-5 (f) Data for NVS-ZP7-6 (g) Data for NVS-ZP7-7 (h) Data for NVS-ZP7-8.

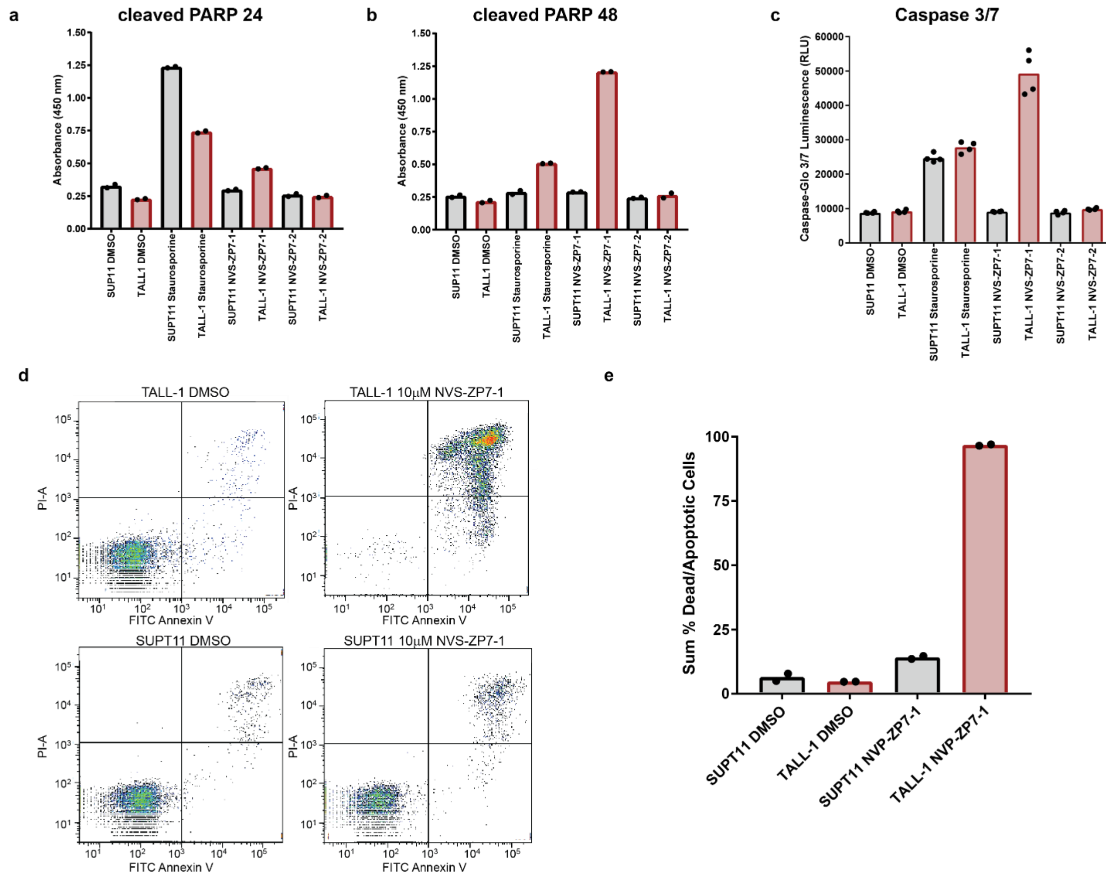

Supplementary Figure 2. NVS-ZP7-1 induces apoptosis in multiple assay formats. (a) Induction of cleaved PARP Elisa following DMSO, 10μM NVS-ZP7-1, 10μM NVS-ZP7-2 and 10μM staurosporine for 24hrs. (b) Induction of cleaved PARP Elisa following DMSO, 10μM NVS-ZP7-1, 10μM NVS-ZP7-2 and 10μM staurosporine for 48hrs. Supplementary figures 2a and 2b represent the cleaved PARP absorbance data from one individual experiment in which 2 independent samples are treated with compound. The average readout value for these samples is represented by the dot-plot bar graph. Each experiment was performed 2 independent times. (c) Induction of Caspase-Glo 3/7 activity following DMSO, 10μM NVS-ZP7-1, 10μM NVS-ZP7-2 and 10μM staurosporine for 48hrs. The bar graph represents the caspase-glo 3/7 luminescence data from one individual experiment in which 4 independent samples are treated with compound. The average readout value for these samples is represented by the dot-plot bar graph. Each experiment was performed 2 independent times. (d) FACS plots of PI and FITC annexin V staining gated into quadrants for cells treated with either DMSO or 10μM NVS-ZP7-1. Refer to Supplementary figure 14 for example gating strategy used for PI and FITC annexin V

FACS assay. (e) Sum of % of Dead and % Apoptotic cells from (d) represented as a bar graph. Data shown is an increase in % of dead and apoptotic cells by annexin V/PI staining after compound treatment. Each bar graph represents the data from one individual experiment in which 2 independent samples are treated with compound. The average readout value for these samples is represented by the dot-plot bar graph. Each experiment was performed 2 independent times.

a

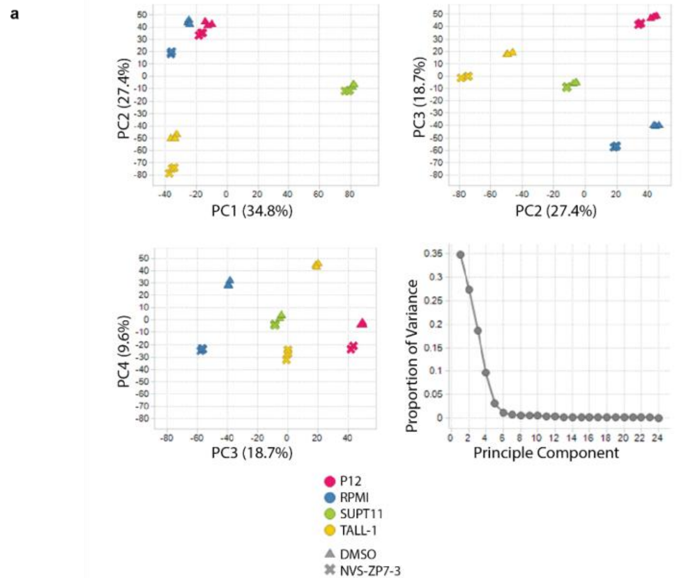

b

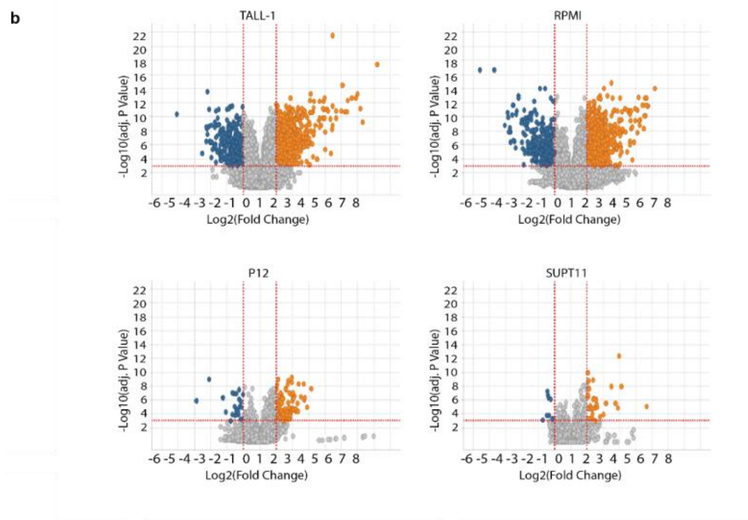

Supplementary Figure 3. Transcriptional changes induced by NVS-ZIP7-3 are greater in sensitive than resistant cell lines. (a) Principle component analysis summary showing scatter plots for the first four components, which account for 90.5% of the variance observed. Each point on the plot represents one sample colored by cell line identity and shaped by treatment. Note that biological replicates group closely together, and that the distance between DMSO-

treated and NVS-ZIP7-3-treated samples for each cell line is greater for sensitive cell lines than for insensitive cell lines. (b) Univariate statistical analysis of each cell line comparing treated to vehicle controls. Scatter plots for each cell line show distribution of probe sets with the x-axis indicating Log2 (Fold Change) and the y-axis the adjusted P-value derived from the moderated T-statistic. The vertical dotted red lines define significant effect size threshold of $|\text{Fold Change}| > 2$ and the horizontal dotted red line defines the adjusted p-value significance threshold of $adj.P < 0.001$.

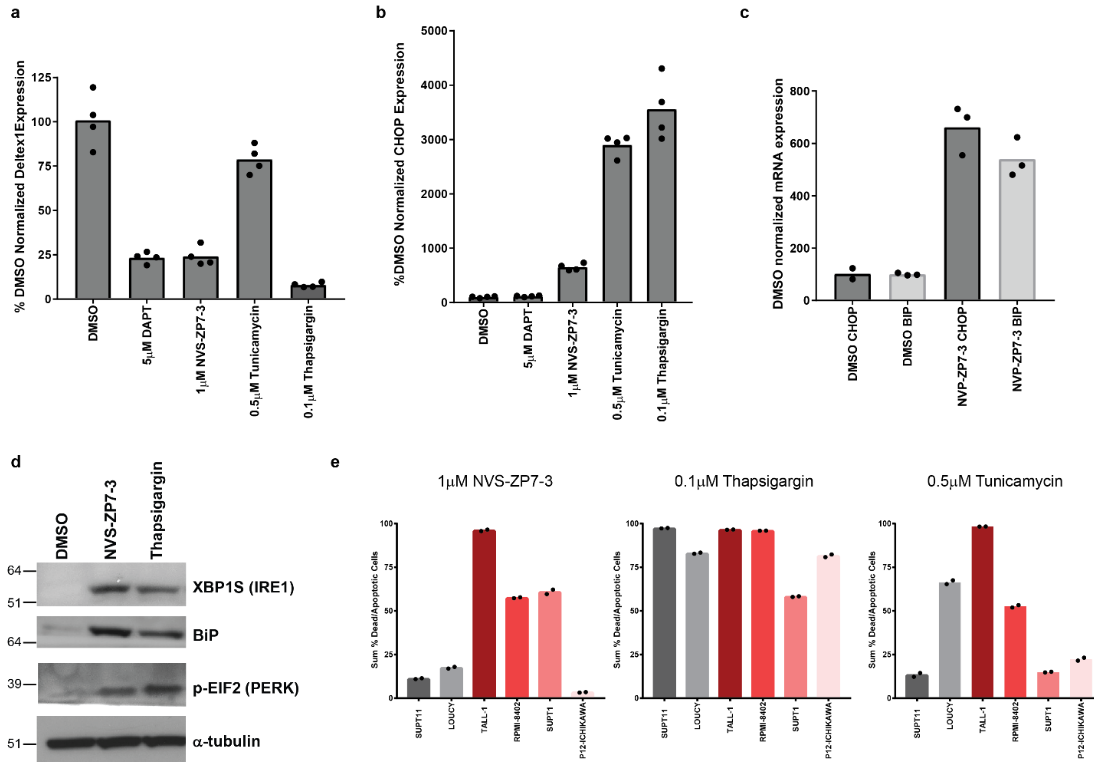

Supplementary Figure 4. Induction of ER stress mRNA and protein readouts in RPMI-8402 cells. (a) *Deltex1* (Notch target gene) mRNA expression following treatment with either DMSO, DAPT (gamma secretase inhibitor), NVS-ZP7-3, tunicamycin or thapsigargin for 8hrs. (b) *CHOP* (ER stress target gene) mRNA expression following treatment with either DMSO, DAPT (gamma secretase inhibitor), NVS-ZP7-3, tunicamycin or thapsigargin for 8hrs. DMSO normalized gene expression in supplementary figures 4a, b and c represent the data for the technical replicates of the compound treated samples from one individual experiment. The average readout value for these samples is represented by the dot-plot bar graph. Each experiment was performed 2 independent times. (c) ER stress target gene mRNA expression in a Notch 1 mutant T-ALL cell line. RPMI-8402 cells were treated with 1 μM NVS-ZP7-3 for 16hrs. DMSO normalized gene expression is plotted for *BIP* and *CHOP*. (d) Protein levels of ER stress markers in RPMI-8402 cells. Cells were treated with DMSO, 1μM NVS-ZP7-3 or 0.1μM thapsigargin for 4hrs. Spliced XBP1S and p-EIF2 are markers of induction of the IRE1 and PERK arms of the ER stress pathway. The experiment was performed 2 independent times and representative Westerns are shown. Full length gels are shown in Supplementary Figure 14. (e) Increase in % of dead and apoptotic cells by annexin V/PI staining after 72hrs of 1μM NVS-ZP7-

3. 0.1μM thapsigargin, or 0.5μM tunicamycin. Notch pathway active T-ALL cell lines are indicted in shades of red, while Notch pathway inactive cell lines are shown in black/grey. Data shown is an increase in % of dead and apoptotic cells by annexin V/PI staining after compound treatment. Each bar graph represents the data from one individual experiment in which 2 independent samples are treated with compound. The average readout value for these samples is represented by the dot-plot bar graph. Each experiment was performed 3 independent times.

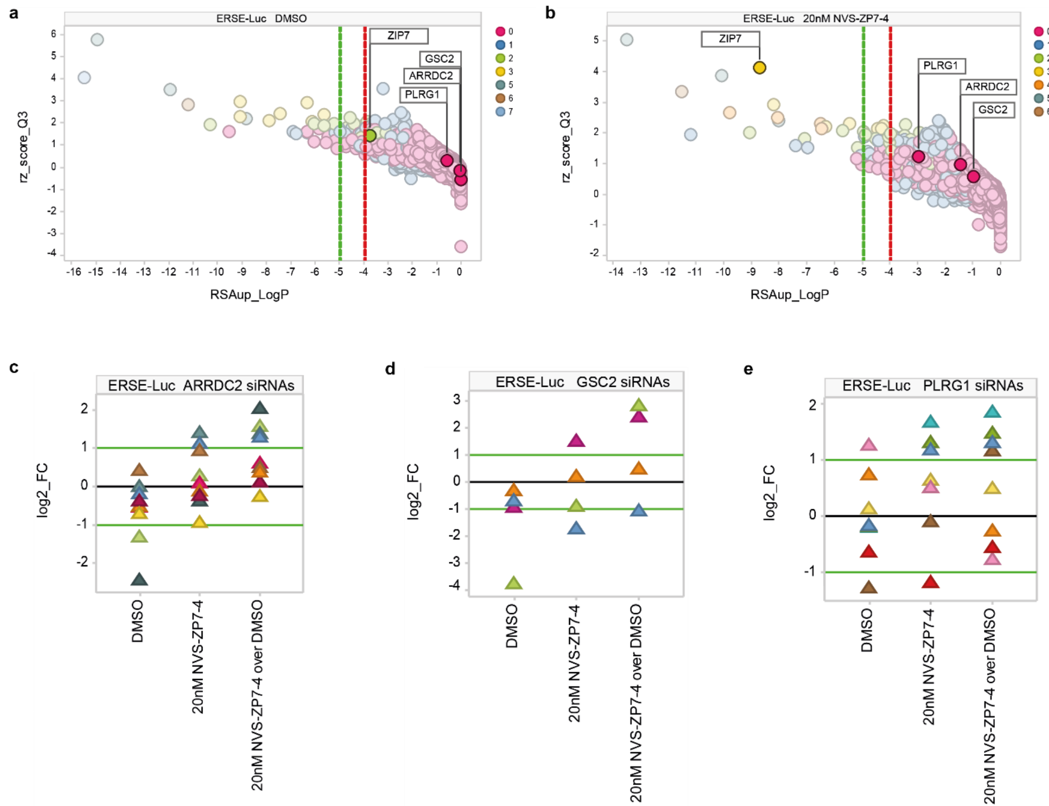

Supplementary Figure 5. Gene level activity in the ERSE-luc genome-wide siRNA screen. (a) Gene level on-target activity in the ERSE-luc assay on the agonist side (increased signaling) was plotted as the gene quartile Q3, as a function of the RSA up log10 p-value (see materials and methods) for the DMSO control. The gene rz_score Quartile Q3 was plotted as a function of the gene RSA up log10 p-value. Stringent (green line) and loose (red line) significance thresholds of RSA log10 p-value were determined by performing and RSA/Quartile analysis on the dataset with the gene id randomized. Color was set to depict the number of siRNAs per gene where activity (robust z-score) was above +2. (b) Gene level on-target activity in the ERSE-luc assay on the agonist side for 20nM NVS-ZP7-4. Analysis as in (a). (c-e) The log2_Fold change activity in the ERSE-Luc assay of the siRNAs for the subset of genes highlighted in Figure 4d are represented as a function of each screening condition.

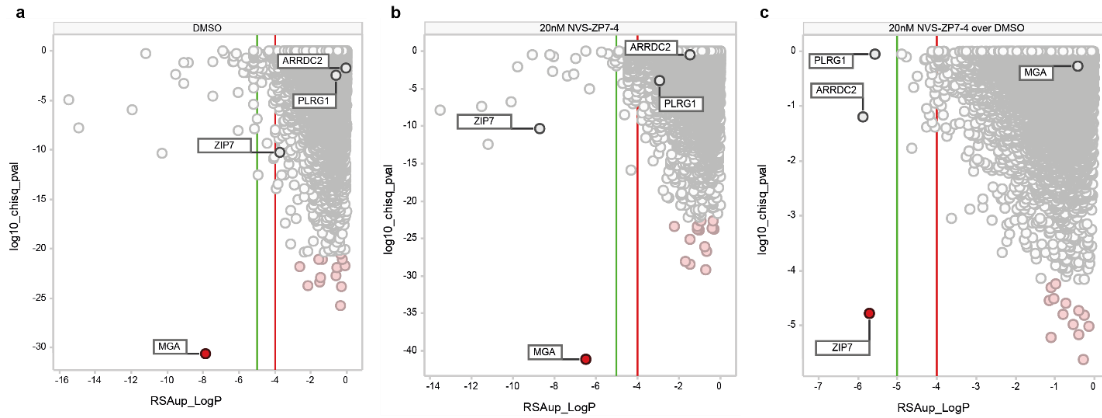

Supplementary Figure 6. On and off-target activity in the ERSE-luc genome-wide siRNA screen. The GESS model off-target statistic (Chi-squared log10 p-value) was plotted as a function of the on-target statistic RSA log10 p-value on the agonist side (increased signaling) for the individual screening conditions (a) DMSO (b) 20nM NVS-ZP7-4 (c) Differential 20nM NVS-ZP7-4 over DMSO. The stringent and loose thresholds of significance estimated by parallel RSA/Quartile determination on randomized data sets are represented as green (RSA up log10 p-value <-5) and red (RSA up log10 p-value <-4) respectively.

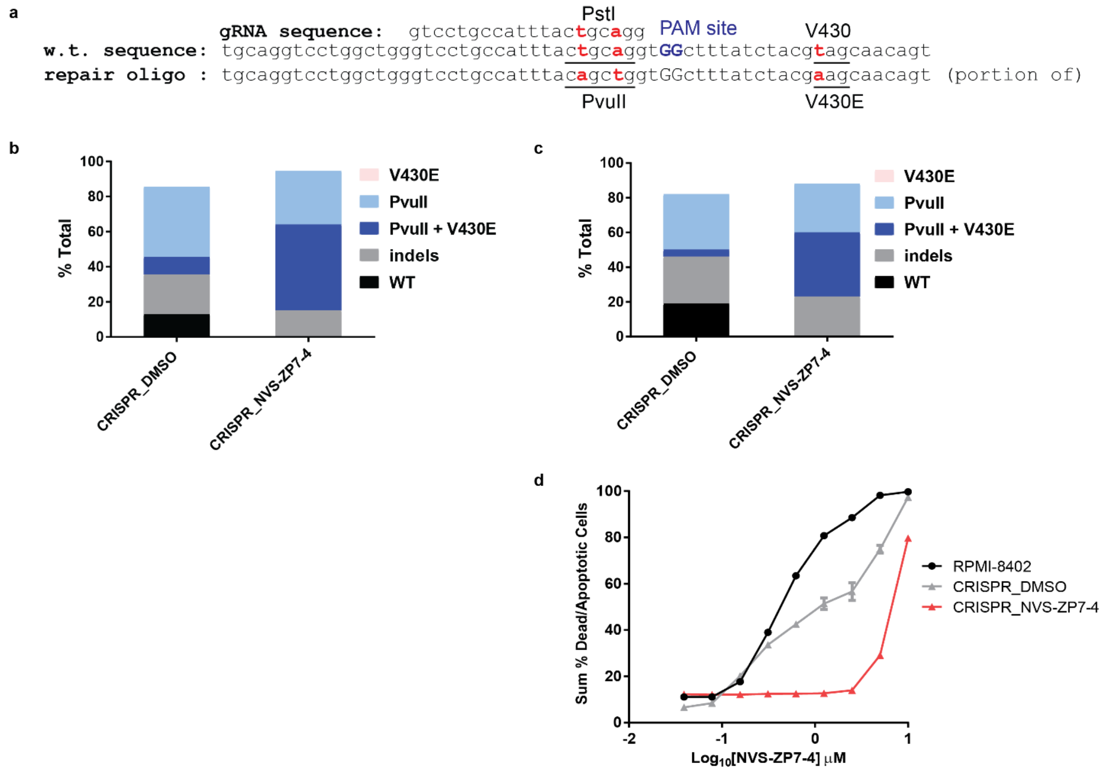

Supplementary Figure 7. CRISPR to introduce ZIP7 V430E mutation. (a) Schematic of targeting strategy to introduce ZIP7 V430E mutation including wild-type ZIP7 sequence, sequence of a portion of the repair oligo, CRISPR PAM site and the guide RNA (gRNA). Restriction enzyme sites for Pst1 and PvuII as well a sequence encoding V430 and E430 are shown. (b) TALL-1 cell line abundance of different alleles in control (CRISPR_DMSO) and compound treated samples (CRISPR_NVS-ZP7-4) based on next generation amplicon sequencing. WT denotes wild-type reads while indels refers to other insertions or deletions beyond in-frame repair to PvuII, V430E or PvuII + V430E. (c) RPMI-8402 cell abundance of different alleles in control (CRISPR_DMSO) and compound treated samples (CRISPR_NVS-ZP7-4) based on next generation amplicon sequencing. WT denotes wild type reads while indels refers to other insertions or deletions beyond in-frame repair to PvuII, V430E or PvuII + V430E. (d) Effect of 72hrs of NVS-ZP7-4 treatment on apoptosis/cell death as measured by annexin V/PI staining in RPMI-8402 cells, as well as RPMI-8402 cells following introduction of the ZIP7 V430E mutation with CRISPR and short-term selection with either DMSO (CRISPR_DMSO) or NVS-ZP7-4 (CRISPR_NVS-ZP7-4). Data shown is an increase in % of dead and apoptotic cells by annexin V/PI staining after compound treatment. The XY line graph

represents the data from one individual experiment in which 2 independent samples are treated with compound. The average readout value for these samples is represented by the points and connecting lines with standard error bars. This exact experiment was performed 2 independent times.

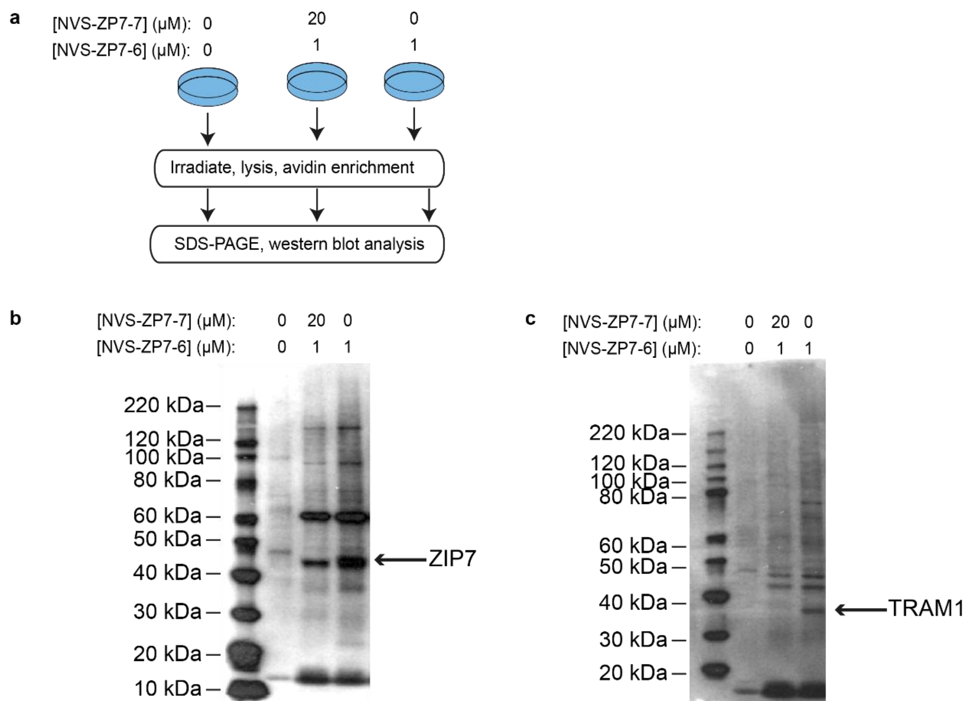

Supplementary Figure 8. Western blot validation of select targets identified from de novo photoaffinty labeling experiment (a) Schematic overview of PAL probe titration strategy. Cells were initially treated with 20 μM NVS-ZP7-7 or vehicle for 1 hr. After the 1 hr incubation, cells were treated with NVS-ZP7-6 or vehicle for 1 hr. After incubation with the photoaffinity probe, cells were irradiated, lysed and subjected to avidin enrichment as previously described. (b) Western blot analysis of ZIP7 and (c) TRAM1 demonstrate that both proteins are enriched over samples treated not treated with the photoaffinity probe (NVS-ZP7-6) and that this enrichment could be competed by pre-incubation with NVS-ZP7-7. The experiment was performed two independent times and representative Westerns are shown.

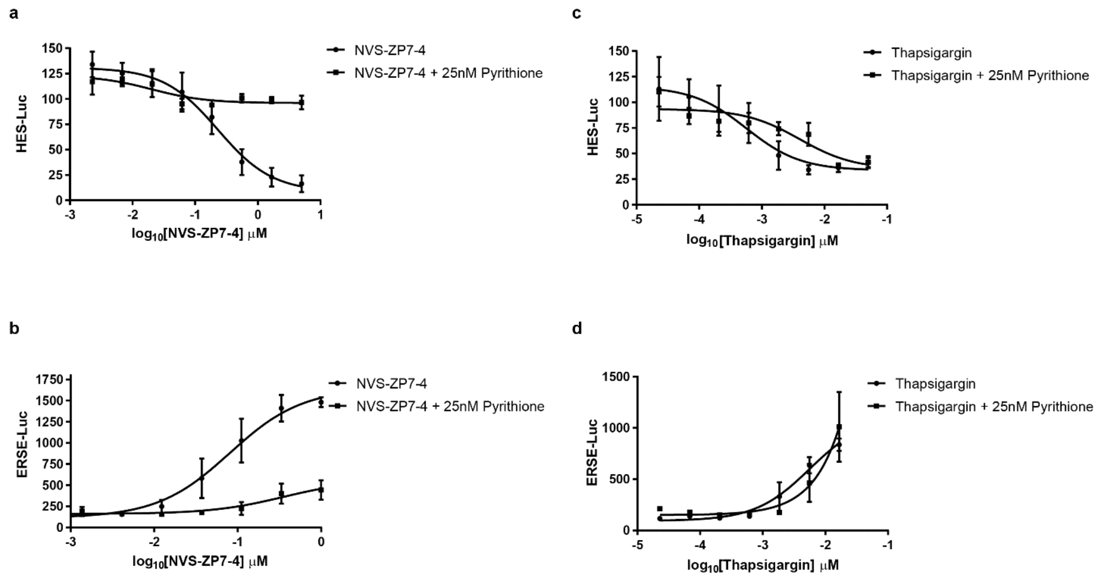

Supplementary Figure 9. Co-treatment with the zinc ionophore, pyrithione, rescues the effects of NVS-ZP7-4 but not thapsigargin in HES-Luc and ERSE-Luc assays. (a) Dose response of NVS-ZP7-4 or NVS-ZP7-4 + 25nM pyrithione in the Notch signaling, HES-Luc assay. 25nM pyrithione was selected for all combination studies in both reporter gene assays, as at this dose it has no effect on its own in the HES-Luc or ERSE-Luc assay. (b) Dose response of NVS-ZP7-4 or NVS-ZP7-4 + 25nM pyrithione in the ER stress, ERSE-Luc assay. (c) Dose response of thapsigargin or thapsigargin + 25nM pyrithione in the Notch signaling, HES-Luc assay. (d) Dose response of thapsigardin or thapsigargin + 25nM pyrithione in the ER stress, ERSE-Luc assay. Error bars represent standard deviation of the mean from 6 biological replicates (n=6) in an individual experiment. Each experiment was performed 3 independent times.

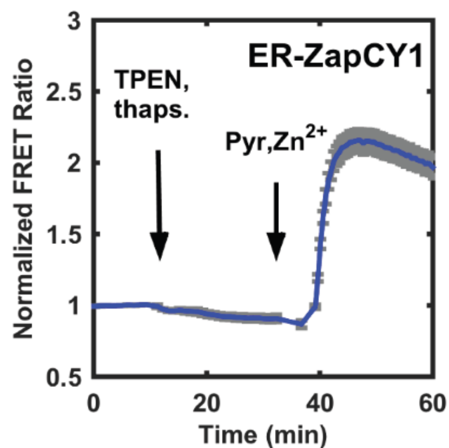

Supplementary Figure 10. Sensor calibrations determine the response range of ER-ZapCY1. U2OS cells (n = 18), were transfected with ER-ZapCY1 24 hours before imaging. In the ER, ER-ZapCY1 exhibits a small decrease in FRET ratio when treated with the membrane permeable metal chelator N,N,N',N'-tetrakis-(2-pyridylmethyl)-ethylenediamine (TPEN, 150 μM) and thapsigargin (thaps., 10 μM), followed by an increase upon saturation with the ionophore pyrithione (Pyr, 0.75 μM) and Zn2+ (12 μM). This sensor displays an approximately 2.2-fold increase in FRET ratio upon Zn2+ saturation. FRET ratios were normalized to the average FRET ratio of each cell before compound treatment. Error bars are the standard error of the mean for one individual experiment.

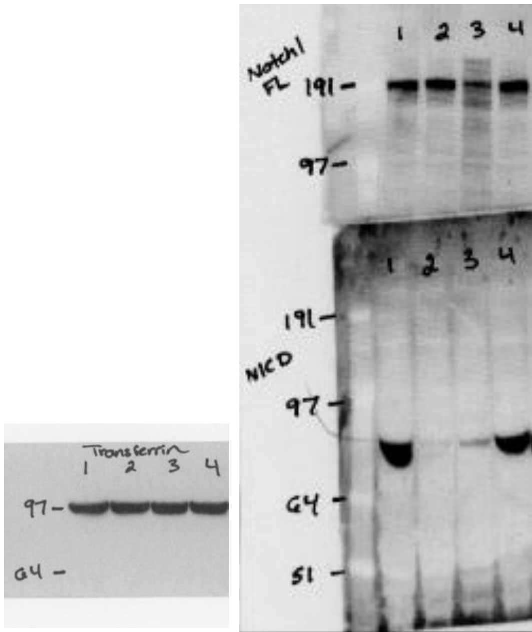

Supplementary Figure 11. Uncropped Western blots for Figure 1d. Sample 1: DMSO, Sample 2: DAPT, Sample 3: NVS-ZP7-1, Sample 4: NVS-ZP7-2

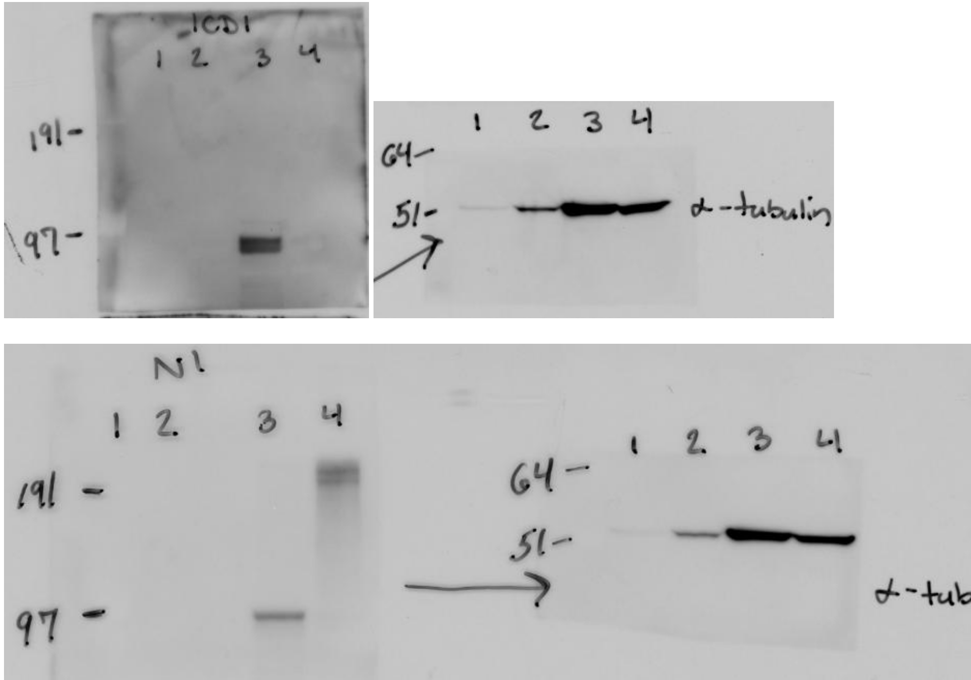

Supplementary Figure 12. Uncropped Western blots for Figure 1e. Sample 1: not applicable, Sample 2: not applicable, Sample 3: DMSO, Sample 4: NVS-ZP7-3

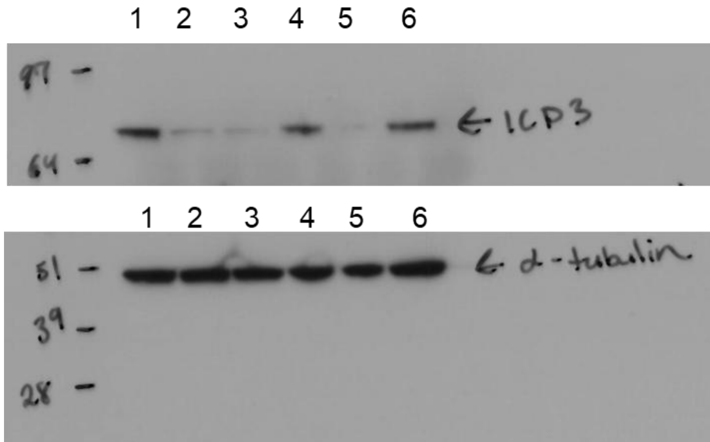

Supplementary Figure 13. Uncropped Western blots for Figure 3b. Sample 1: DMSO-parental, Sample 2: DAPT-parental, Sample 3: NVS-ZP7-4-Parental, Sample 4: DMSO-Resistant, Sample 5: DAPT-resistant, Sample 6: NVS-ZP7-4-Resistant

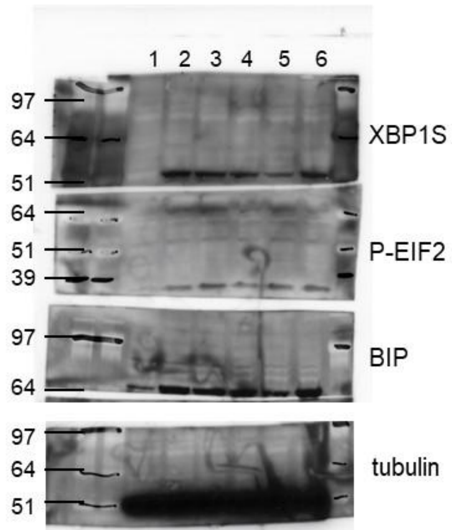

Supplementary Figure 14. Uncropped Western blots for Supplementary Figure 4d. Sample 1: DMSO, Sample 2: NVS-ZP7-3, Sample 3: Thapsigargin, Sample 4, 5, 6: not applicable

Step 1: Forward/side scatter to gate single cells

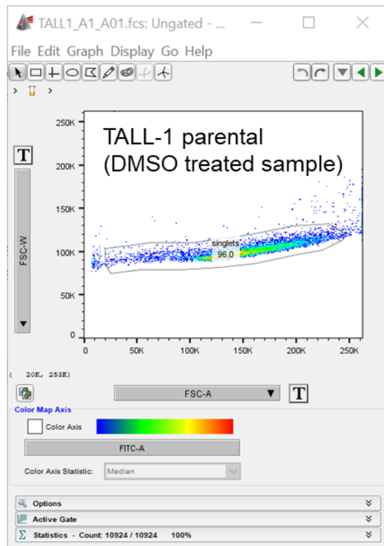

Step 2: Setting up gating quadrants for cell debris (Q1), dead (Q2), apoptotic (Q3), live (Q4)

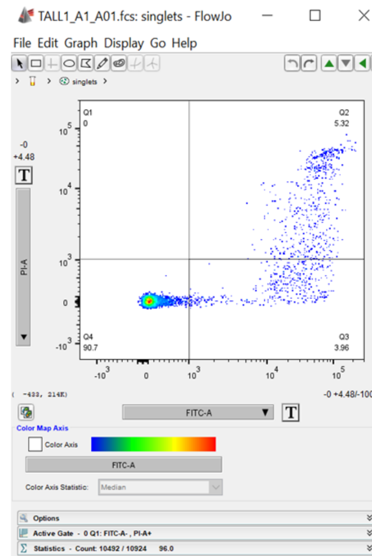

Step 3: Exported statistics for all samples into excel which was used to calculate the sum of the percent dead and apoptotic cells. These values were then put into Graph Pad Prism to generate the dot-plot bar graphs in Figures 2a and 3a and supplementary figures 2e and 4e. The same set of values were put into Graph Pad Prism to generate the XY line graphs in Figure 5b and supplemental figure 7d. The example flow analysis shown here is one of the two DMSO treated TALL-1 parental samples from the experiment shown in Figure 3a.

Name	Statistic	#Cells
TALL1_A1_A01.fcs		10924
singlets	96.0	10492
Q1: FITC-A- , PI-A+	0	0
Q2: FITC-A+ , PI-A+	5.32	558
Q3: FITC-A+ , PI-A-	3.96	416
Q4: FITC-A- , PI-A-	90.7	9518

Formatted: Font: (Default) Arial, Bold

Supplementary Figure 15. FACS gating strategy for representative Vybrant apoptosis assay

Supplementary Figure 16. Schematic of pXP1510 cloning vector

Position	All_AACHANGE	GenomicChange	Frequency of mutation
100	S100G	298A>G	2.09%
173	**L173F**	**517C>T**	**5.97%**
173	L173P	518T>C	4.75%
176	A176T	526G>A	2.06%
180	L180F	538C>T	4.92%
230	**F230S**	**689T>C**	**9.20%**
244	H244R	731A>G	1.72%
328	A328V	983C>T	2.11%
332	T332A	994A>G	3.15%
365	G365E	1094G>A	1.59%
427	**F427L**	**1279T>C**	**7.52%**
429	Y429H	1285T>C	6.44%
430	V430I	1288G>A	3.92%
435	V435M	1303G>A	3.51%
439	L439P	1316T>C	4.37%
440	L440P	1319T>C	5.68%

Supplementary Table 1. Frequency and location of mutations in ZIP7 following variomics experiment and selection with 10μM NVS-ZP7-5

Cell Line	Notch1 HD	Notch1 PEST	Other
HPB-ALL[1]	L1575P (heterozygous)	2444 heterozygous insertion	
TALL-1[2]	Wild-type	Wild-Type	Notch3 S1580L
RPMI-8402[1]	1584 heterozygous insertion	Wild-Type	
PF382[1]	L1575P (heterozygous)	2494 heterozygous insertion	
Loucy[1]	Wild-Type	Wild-Type	
SUPT1[1]			t(7;9)(q34;q34.3) translocation
SUPT11[1]	Wild-Type	Wild-Type	
P12-Ichikawa[1]	12 amino acid insertion in HD domain		

Supplementary Table 2. T-ALL cell line Notch mutation status

Notch mutation status is described in the following manuscripts

1. Weng, A.P. et al. Activating mutations of NOTCH1 in human T cell acute lymphoblastic leukemia. *Science* **306**, 269-71 (2004).
2. Bernasconi-Elias, P. et al. Characterization of activating mutations of NOTCH3 in T-cell acute lymphoblastic leukemia and anti-leukemic activity of NOTCH3 inhibitory antibodies. *Oncogene* **35**, 6077-6086 (2016).

Gene	ABI Taqman Probe
Deltex1	Hs00269995_m1
Notch3	Hs01128541_m1
CHOP	Hs01090850_m1
BiP	Hs00946084_g1
PP1A	Hs99999904_m1

Supplementary Table 3. ABI Taqman Probes for mRNA quantitation

Protein	Antibody	Use and Dilution
Anti-Notch1 antibody, extracellular domain	Millipore Sigma Catalog # 07-218	Western 1:1000
Notch1 (5B5) Rat mAb (detects FL and TM-ICD)	Cell Signaling, Catalog # 3447	Western 1:500
Cleaved Notch1 (Val1744) (D3B8) Rabbit mAb	Cell Signaling, Catalog # 4147	Western 1:250 or 1:500
Human TfR (Transferrin R) Antibody	R&D Systems , Catalog # AF2474	FACS 10μl
Transferrin Receptor Monoclonal Antibody (H68.4)	ThermoScientific Catalog # 13-6800	Western 1:500
α-tubulin mouse monoclonal	Sigma Aldrich - #T6199	Western 1:10000
XBP-1s	Biolegend #647502	Western 1:250
BiP (C50B12) Rabbit mAb	Cell Signaling Technologies #3177	Western 1:1000
p-EIF2α (Ser51)	Cell Signaling Technologies # 9721	Western 1:1000
TRAM1	Abcam ab96106	Western 1:1000
SLC39A7/ZIP7 (D1O3A)	Cell Signaling Technologies #33176S	Western 1:1000
Notch3 Intracellular domain	Custom ICD3 Antibody	Western 1:500
donkey anti-rabbit IgG conjugated to horseradish peroxidase	Amersham Cat#NA9340V	Western 1:10000
sheep anti-mouse IgG conjugated to horseradish peroxidase	Amersham Cat# NA931V	Western 1:10000

Supplementary Table 4. Antibodies for FACS and Western blotting

Custom ICD3 antibody generation is described in the following reference[1]

1. Bernasconi-Elias, P. et al. Characterization of activating mutations of NOTCH3 in T-cell acute lymphoblastic leukemia and anti-leukemic activity of NOTCH3 inhibitory antibodies. *Oncogene* **35**, 6077-6086 (2016).

Name	Details	Sequence
Dh1-Zip7 siRNA	Dharmacon On-Targetplus SLC39A7 siRNA J-007338-17	Target Sequence 5'- CAUCAAACAUCAAUCGUGU- 3'
Qi1-Zip7 siRNA	Qiagen Hs_SLC39A7_4FlexiTube siRNA SI00724668	Target Sequence 5'- ATGGAAGACAAGAGCGTTCTA- 3'
Dh2 siRNA	Dharmacon On-Targetplus SLC39A7 siRNA J-007338-18	Target Sequence 5'- GAAAUAAAGACCUCCGAUC- 3'
Dh3 siRNA	Dharmacon On-Targetplus SLC39A7 siRNA J-007338-20	Target Sequence 5'- GACAAGAGCGUUCUACCAA- 3
Neg1	Dharmacon Neg 1 siRNA D-001810-01	
Neg3	Dharmacon Neg 3 siRNA D-001810-03	
pGL3		Target Sequence 5'- CTTACGCTGAGTACTTCGA- 3'
pGL2		Target Sequence 5'- CGTACGCGGAATACTTCGA- 3'
pGL4		Target Sequence 5'- AAGAAGTGCTCGTCCTCGTCC- 3'

Supplementary Table 5. siRNA sequences

Category	Parameter	Description
Assay	Type of assay	U2OS Notch ICD inducible Hes-Luc Reporter Gene Assay (RGA)
	Target	Notch
	Primary measurement	Luminescence measurement (Luciferase activity) 30 hours post compound addition
	Key reagents	Bright Glo (Promega), U2OS Tet-On ICD4 A48 cell line
	Assay protocol	4K cells per well plated in 384 well plates in 25uL using a Matrix Wellmate. Incubate O/N at 37ºC 5% CO_2 10uM final concentration of compound was added to cells (5uL/well) using a BiomekFX 2ug/mL Doxycycline was added to wells (5uL/well) using a Matrix Wellmate Plates incubated at 37ºC 5%CO_2 for 30 hrs Post incubation Bright Glo:Water (1:1) (30uL/well) was added and plates were incubated at RT for 5 minutes Plates read on Viewlux Imager with an exposure time of 30 sec
	Additional comments	A stable cell line expressing a Notch reporter gene, HES-Luciferase, as well as the Tet-inducible intracellular domain (ICD) of Notch 4 was created and used for this screen. Treatment of the cells with Doxycycline, leads to the production of ICD and activation of the HES-Luciferase reporter. Luciferase activity levels are monitored by adding the substrate luciferin and reading the amount of light produced.
Library	Library size	1,155,264
	Library composition	(Random) screening deck
	Source	Novartis compound library
	Additional comments	
Screen	Format	384 well

	Concentration(s) tested	10uM
	Plate controls	DMSO (0.5%), no dox well
	Reagent/ compound dispensing system	Flexdrop (Perkin Elmer) for dilution, VPrep to deliver compounds to cells
	Detection instrument and software	Viewlux Imager
	Assay validation/QC	Z' value above 0.8 and a signal window greater than 7 fold (luc signal for dox vs no dox).
	Correction factors	Helios (Novartis internal) analysis software as needed for well masking or correction
	Normalization	Plate-based robust Z
	Additional comments	
Post-HTS analysis	Hit criteria	50% inhibition
	Hit rate	4.1% primary, 2.8% post *in silico* triaging
	Additional assay(s)	Validation: 8-point dose response HES-RGA; Secondary assays: Notch Target Gene qRT-PCR; Counterscreen for cytotoxicity: U2OS TRE Luc Tet-On RGA
	Confirmation of hit purity and structure	LC/MS
	Additional comments	Compound hits were triaged (Pipeline Pilot) using chemical unattractiveness, reactivity, and promiscuity filters

Supplementary Table 6. High through-put screen small molecule screening data